Zornoza, A., Olier, D., Sagues, M., & Loayssa, A. (2010). Brillouin distributed sensor using RF shaping of pump pulses. Measurement Science and Technology. https://doi.org/10.1088/0957-0233/21/9/094021

Brillouin distributed sensor using RF shaping of pump pulses

Ander Zornoza, David Olier, Mikel Sagues and Alayn Loayssa
Departamento de Ingeniería Eléctrica y Electrónica, Universidad Pública de Navarra, Pamplona, Spain,

E-mail: ander.zornoza@unavarra.es

Abstract

We introduce a novel configuration for long-range Brillouin optical time domain analysis (BOTDA) sensors that is based on shaping the pump pulses in the radio frequency instead of the optical domain. This results in a simplified setup that uses just one standard intensity modulator to generate pulses with extremely high extinction ratio (60dB in our experiments). We develop a theoretical model for Brillouin interaction in long-distance BOTDA and use simulations to demonstrate that the availability of such pure pulses completely suppresses measurement errors caused by pulse leakage. Finally, experimental results are shown to confirm theoretical predictions. A 25-km fibre is measured with our system and the results compared to those obtained using pump pulses with lower extinction ratios.

Keywords: Brillouin fibre sensing, distributed fibre sensor, stimulated Brillouin scattering, BOTDA.

Submitted to Measurement Science and Technology

1. Introduction

In 1989 it was demonstrated for the first time that distributed measurements could be performed in an optical fibre by the so-called Brillouin optical time domain analysis (BOTDA) [1]. This technique exploits the stimulated Brillouin scattering (SBS) dependence on temperature and strain [2]. Hence, much research has been devoted to BOTDA sensors in recent years. However, there are still unresolved issues that hinder widespread adoption of this technology.

Current research in BOTDA sensors is divided in two main areas. The first one is high-resolution sensors, with centimetre spatial resolutions, but only capable to perform measurements in relatively short-distance fibres. Research on these sensors is focused on devising techniques to overcome the physical limits imposed by the phonon lifetime. The work presented in this paper relates to the second main area of research, long-range BOTDA sensors, which are able to perform measurements in tenths of kilometre fibres with meter resolutions.

The main challenges in long-range sensing are to simplify the setups, to increase the sensing range and to compensate measurement errors caused by non-local effects. Most BOTDA implementations are complex and use expensive components such as multiple electro-optic modulators, semiconductor optical amplifiers,

synthesized microwave generators or wideband detectors. Therefore, a major line of research in these sensors is to simplify the experimental setups so as to achieve a cost-effective commercial system that can compete, for instance, with the much simpler and less costly distributed Raman sensors for temperature measurements. Some examples of contributions in this area include the deployment of injection locking to generate the pump and probe waves using inexpensive DFB lasers [3], the use of Brillouin generators or Brillouin fibre lasers to obtain the probe wave from the pump [4] or the use of offset-locking [5].

The sensing range of BOTDA is limited by the attenuation of pump pulses and can be compensated in principle by increasing the pump power. However, high pump powers lead to the occurrence of the modulation instability effect, which limits the maximum measurable distance [6]. Using dispersion-shifted fibre [7] or pump pulse coding [8] have been demonstrated to mitigate this effect.

Non local effects mean that the measurement of a fraction of the fibre is affected by the rest of the fibre. They are induced by the pump pulse depletion along the fibre as it interacts with the continuous wave (CW) probe. This causes an error in the measured Brillouin frequency shift that can be partially compensated using additional measurements of the pump pulses [9] or by post processing [10].

Non-local effects are greatly enhanced by imperfections in the generated pump pulses. When optical devices such as optical modulators are used to shape the pump pulse there is always a residual DC base or leakage. Thus, there is SBS interaction between the leakage and probe in addition to that between the pulse and the probe. This leads to a distortion of the measured Brillouin spectra. Solutions to improve extinction ratio (ER) of pump pulses have been proposed using the injection locking method [3], using semiconductor optical amplifiers as optical switches [11] or using specialty ultra-high extinction ratio electro-optic modulators [5].

In this paper we present an alternative solution in the form of a simplified BOTDA sensing scheme that shapes pump pulses in the RF domain, where it is easier and cheaper to obtain high ER pulses [12]. A theoretical model is developed to investigate the effect of leakage in long-range BOTDA sensing and to calculate errors caused by this effect. Then, we experimentally demonstrate our scheme and compare measurement results with those obtained using conventional shaping of the pump pulses.

2. Theoretical model

2.1. Model description

The general scheme of a BOTDA sensor involves two waves that are introduced in a fibre in opposite directions: a pulse pump wave (I_P) and a CW probe wave (I_S). There are basically two different methods to solve the interaction between them. In one hand we have models designed for high spatial resolution BOTDA

systems, which solve the time-domain differential equations that describe the complex interaction between optical and acoustic waves [13]. These are required when we are using pulses whose length is shorter than the lifetime of acoustic phonons. On the other hand, in long-range BOTDA we generally have longer length pulses, thus it is possible to use models which solve the interaction between waves defined by the steady-state coupled intensity SBS equations [14]:

$$\frac{dI_P}{dz} = -g(\nu, z) \cdot I_P \cdot I_S - \alpha \cdot I_P \tag{1}$$

$$\frac{dI_S}{dz} = -g(\nu, z) \cdot I_P \cdot I_S + \alpha \cdot I_S \tag{2}$$

Where α is the fibre attenuation coefficient and $g(\upsilon, z)$ represents the Brillouin gain coefficient, which depends on the frequency shift between pump and probe waves and the temperature and strain characteristics of the fibre:

$$g(\nu, z) = \frac{\gamma \cdot g_0}{\left[2 \cdot \frac{\nu_B(z) - \nu}{\Delta \nu_B} \right]^2 + 1} \tag{3}$$

where γ is a polarization coefficient, g_0 is the Brillouin line centre gain coefficient, ν is the frequency shift between the waves, $\Delta \nu_B$ is the Brillouin line width and $\nu_B(z)$ is the temperature/strain dependent Brillouin frequency shift.

Equations (1) and (2) are usually solved by using a perturbation method in which CW is initially affected only by the fibre loss [14, 6]. This is a valid approximation if the pulsed wave has a very high ER. Otherwise, there is a residual DC base or leakage travelling together with the pulsed beam. In this case, we have an SBS interaction between the leakage and the CW, which distorts the CW intensity value all along the fibre. Some authors consider this effect decoupled from the SBS interaction between pulsed and CW beams [15]. Therefore, the total Brillouin spectrum is the product of two different contributions: pulsed-CW and leakage-CW beams SBS interactions. However, this approximation is just valid for short fibre sensors.

In order to investigate the effect of leakage in long range BOTDA sensors we propose a modified theoretical model that does not require the approximation of decoupled SBS effects. This theoretical model deals with three consecutive SBS interactions. Figure 1 schematically depicts these SBS interactions assuming that the pulse is in the position z of the fibre. The first step is to solve the leakage-CW SBS interaction all over the fibre. Equations (1) and (2) can be solved for two counter propagating continuous waves ($I_P = I_L$ and

$I_S = I_{CW}$). Boundary conditions are the input CW intensity ($I_{CW}(L) = I_{CWL}$) and the input leakage intensity ($I_L(0) = I_{P0} / ER$, where I_{P0} is the input peak intensity of the pulsed beam). This method will provide a numeric solution for the CW after interacting with the leakage over the whole fibre length, $I_{CW}(z)$. The effect of this interaction is increasing the CW power at each fibre position when the BOTDA system works in gain configuration.

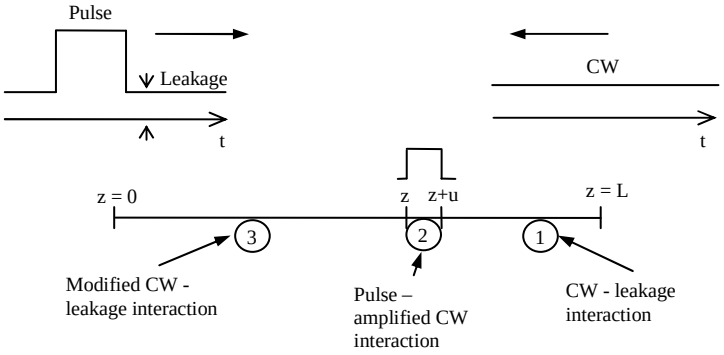

Figure 1: Scheme of the three different SBS interactions considered by the theoretical model.

Substituting this amplified CW expression in (1), as probe wave, we can get a numeric solution for the evolution of the pulsed wave power (I_P) as follows:

$$I_P(\nu, z) = I_P(0) \cdot Exp\left[\int_0^z -g(\nu, z) \cdot I_{CW}(\nu, z) dz - \alpha \cdot z \right] \tag{4}$$

Substituting (4) in (2) and integrating over the interaction region between the pulsed and the amplified CW waves, u , we can obtain the expression for the gain experienced by the CW due to SBS interaction with the pump pulse at position z. The interaction region, u , is defined by half the pulse length and gives the system spatial resolution. The result is:

$$G(\nu, z) = \frac{I_{CW}(\nu, z)}{I_{CW}(\nu, z+u)} = Exp\left\{ - \int_z^{z+u} g(\nu, z) I_P(0) \cdot Exp[I_P(\nu, z)] + \alpha \cdot u \right\} \tag{5}$$

Then, the CW intensity value after interacting with the leakage and the pulsed beam can be obtained as follows:

$$I_{CW}(\nu, z) = I_{CW}(\nu, z+u) \cdot G(\nu, z) \tag{6}$$

Where $I_{CW}(\nu, z+u)$ represents the location in the fibre where the leading edge of the pulse meets the CW wave front.

As we are looking for a received power expression, another SBS interaction between the new modified CW, $I_{CW}(\nu, z)$, and the leakage must be considered in the region after the interaction with the pulsed beam. This can be solved by using the same method as above for $I_P = I_L$ and $I_S = I_{CW}$ with CW intensity in z position ($I_{CW}(\nu, z) = I_{CW}(\nu, z+u) \cdot G(\nu, z)$) and the input leakage intensity ($I_L(0) = I_{P0} / ER$) as boundary conditions. This gives the received power of the interaction between CW, leakage and pulsed beams related to a particular spatial position, z. The pulsed wave propagates along the fibre, so the Brillouin gain signal can be obtained by repeating this process for successive pulse interaction lengths, u, from $z = 0$ to L.

2.2. Leakage-induced distortion

The presence of leakage raises the power of the CW wave, as it has been explained above. Therefore, the power transference between pulsed and CW waves is increased. This change in pulse power alters the measured SBS spectra inducing an error which limits sensor resolution [10].

In order to study the leakage effect, a number of simulations were performed for a 25-km length of standard single mode fibre. A typical measurement of distributed Brillouin spectra along the whole fibre, as simulated by our model, is presented in figure 2. It shows the worst case scenario in which a small section with different Brillouin frequency shift is situated at the end of a fibre with uniform frequency shift. Figure 3 displays the spectra measured at this final section for several Brillouin frequency shifts and two different ER values. Figure 3(a) shows the spectra that was calculated assuming pump pulses with a high ER of 40dB. Notice that the main gain contribution in this case is provided by the interaction of the pulse and CW. However, despite the fact that a large ER is used, the leakage-CW contribution is also noticeable. Thus, the gain maxima are located at the Brillouin frequency shift of the heated section, ν_{B2}, and a small bump is noticed located at the frequency shift of the rest of the fibre, ν_{B1}. Figure 3(b) depicts the spectra assuming a lower ER of 26dB. The main contribution to these spectra is provided by the interaction between leakage and CW, which is caused by this reduced ER. In fact, this SBS interaction hides the pulse-CW contribution of the short final section of the fibre, severely distorting the measured spectra because the gain maxima is always located in the frequency shift of the rest of the fibre, ν_{B1}.

When low ER pulses are used we can perform a correction of the measured spectra. In order to minimize the leakage contribution the spectrum of the interaction when no pulse is present in the fibre can be calculated. This spectrum, $I_{LC}(\nu)$, only depends on the frequency shift between leakage and CW, so its contribution is

not time-dependent and can be threatened as independent from the gain caused by the pulse. Then, to isolate the gain produced by the pulse we define the correction:

$$I(\nu)=\frac{I_M(\nu,z)}{I_{LC}(\nu)} \tag{7}$$

Where $I_M(\nu,z)$ is the measured spectrum. This is similar to the so-called AC detection used in [16], but instead of subtracting the interaction between leakage and CW, we divide by it. This way we separate the gain generated by the pulse. Note that to perform correction (7) properly, all measurements and simulations in this paper require that signals are detected using a photodiode operating with DC coupling. Moreover, when the leakage level is very low, correction (7) is unnecessary because the interaction between leakage and CW is negligible.

Correction (7) applied to spectra of figure 3(b) are shown in figure 4. These spectra show how this correction reduces leakage contribution. However, it is only valid when the pulse depletion due to the additional CW power provided by interaction with the leakage can be neglected. This is not generally the case and thus the compensated spectra of figure 4 have an error in the frequency of the maxima because of this effect. These errors are shown in figure 5 for four values of ER and increasing pump power. It can be seen that leakage increases non local effects due to pump depletion. Therefore, reduction of this leakage is of the essence.

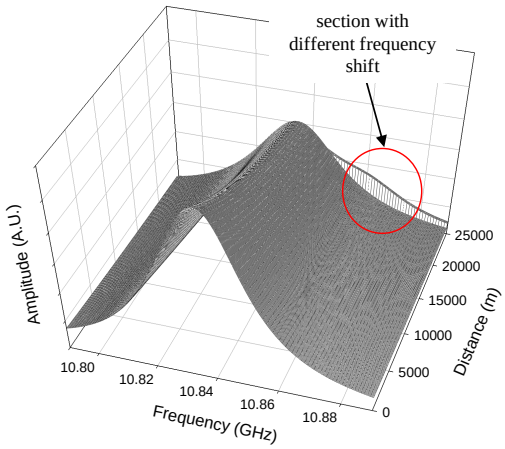

Figure 2: Evolution of the Brillouin spectrum along the fibre. The section with different Brillouin frequency shift (300m-long) is distorted because of the leakage presence. The parameters are: L = 25 km, u = 20 m, P_P = 20 dBm, P_{CW} = -3 dBm, ER = 29 dB.

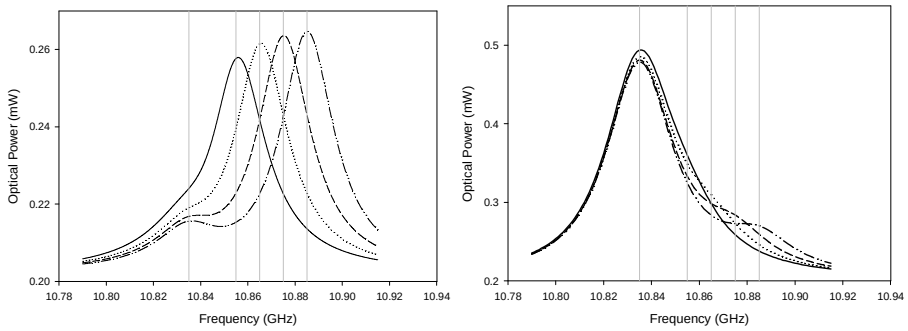

(a) (b)

Figure 3: Brillouin spectra of the 300 m-long sections with different Brillouin frequency shift in a 25 km fibre for ER = 40 dB in case (a) and ER=26dB in case (b). Parameters: L = 25 km, u = 20 m, P_P = 28 dBm, P_{CW} = -2 dBm. Brillouin frequency shift of the rest of the fibre: $\nu_{B1} =$ 10.835 GHz; and for the section with different Brillouin frequency shift: $\nu_{B2} =$10.855 GHz (continuous); 10.865 GHz (dotted); 10.875 GHz (dashed); 10.885 GHz (dot-dot-dash line). These frequencies are marked with a vertical line.

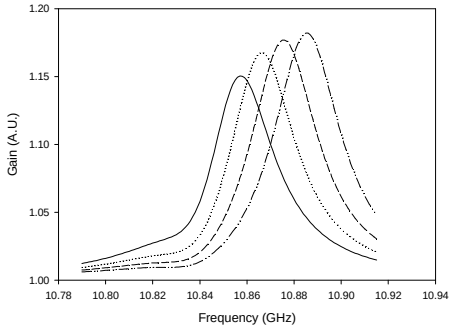

Figure 4: Brillouin compensated spectrum of the 300 m sections with different Brillouin frequency shift in a 25 km fibre. Parameters: L = 25 km, u = 20 m, P_P = 28 dBm, P_{CW} = -2 dBm, ER = 26 dB. Brillouin frequency shift of the rest of the fibre: $\upsilon_{B1} =$ 10.835 GHz; and for the section with different frequency shift: $\upsilon_{B2} =$10.855 GHz (continuous); 10.865 GHz (dotted); 10.875 GHz (dashed); 10.885 GHz (dot-dot-dash line).

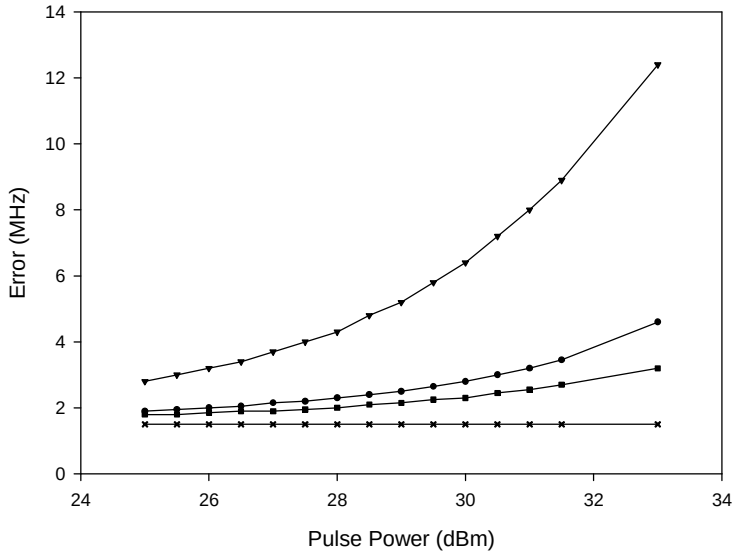

Figure 5: Error in frequency for the worst case scenario depending in launched pump power Pp, for a fixed value of ER. L = 25 km, u = 20 m, PCW = -2 dBm, ER = 21 dB (triangle); 26 dB (circle); 28 dB (square); Infinity (cross).

3. Experimental setup

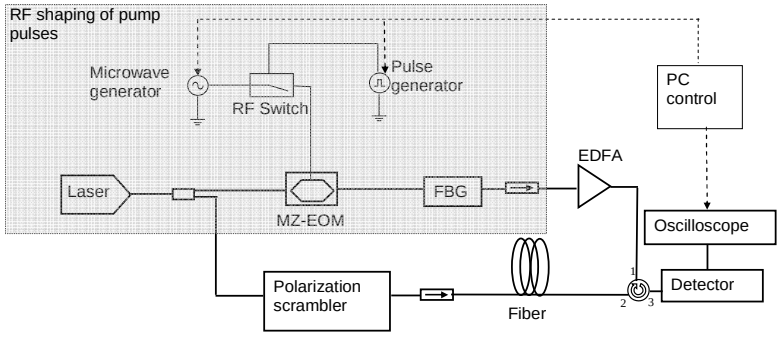

Figure 6: Experimental setup of the proposed high-extinction-ratio and simplified BOTDA sensing scheme. Previously published in [12].

The scheme of our proposed system is shown in figure 6. The output of a single mode laser is first divided in two branches by an optical coupler, so that the same light source is used for pump and Stokes generation. In the upper branch the RF shaping of pump optical pulses is performed, achieving the pulsing and frequency shifting in a single step. The output of the laser is directly used in the lower branch as CW probe.

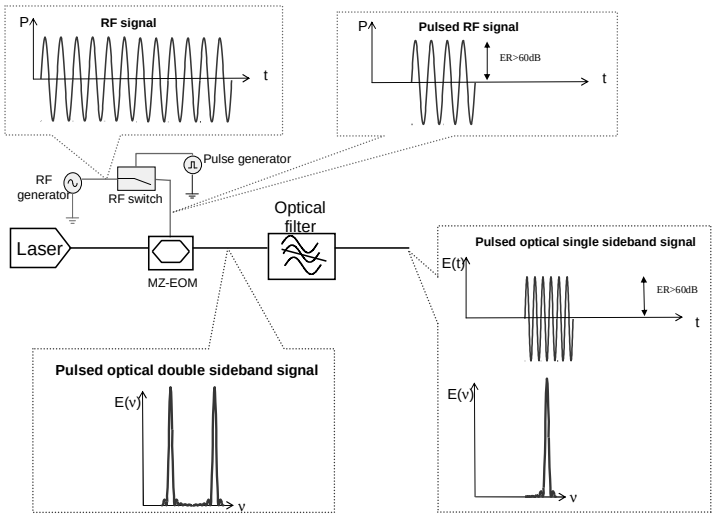

Figure 7: Fundamentals of the RF shaping of optical pump pulses.

In figure 7 the RF shaping of pump pulses is shown in detail. High extinction ratio RF pulses are generated by using a microwave generator, which provides RF signals at frequencies close to the Brillouin frequency-shift in the sensor fibre, followed by a single-pole single-throw microwave switch, which is driven by a pulse generator. Commercial microwave switches are low cost and available with very fast responses (up to 1ns) and extremely high isolation. Therefore, it is possible to obtain fast pulses of RF energy with extremely high extinction ratio. Then a MZ-EOM, operating at the minimum of its transfer curve, is driven by these high-extinction ratio RF pulses. The RF pulse shape is directly translated to the optical domain by the modulator; thus two sidebands pulsed with very high extinction ratio are generated. Then this pulsed optical double sideband suppressed carrier modulation (ODSB-SC) is filtered with a fibre Bragg grating (FBG) to select either the upper sideband, for BOTDA gain configuration, or the lower sideband, if we want to get a Stokes pulse for a BOTDA loss configuration. Therefore, we end up having an ultra-high extinction ratio pump wave. Finally an Erbium-doped fibre amplifier (EDFA) is used to amplify the pulses and apply them to the fibre under test using a circulator.

In the lower branch the laser output is directly used to provide the probe wave. Just a passive polarization scrambler is used to compensate the polarization sensitivity of SBS [6]. The BOTDA signal is directed to a 125-MHz detector by a circulator and is visualized in a digital oscilloscope. A computer is used to control all the instruments by GPIB bus, so it performs the frequency sweep of the RF generator, defines the pulse width and period, captures the BOTDA traces from the oscilloscope and makes the measurement reconstruction.

In conventional BOTDA setups two MZ-EOMs are needed, one to create the CW as a sideband of an ODSB-SC, and another to pulse the pump wave. Furthermore, in order to generate high ER pulses specialty

MZ-EOMs are used, with 45dB ER [5], much more expensive than telecom grade MZ-EOMs, with 20 to 30dB ER. So notice that the presented scheme is different to conventional BOTDA setups, although the pulsing and frequency shift are performed in two steps, only the second one is made in the optical domain, while the pulsing is achieved in the electrical domain. This enables us to create ultra-high extinction ratio pump pulses at low cost, with a RF switch and a single telecom grade MZ-EOM. Moreover, as the CW probe comes directly from the laser with no modulation at all, thus no additional deleterious spurious signals are present in the detected optical spectra and there is no need for additional optical filtering in the receiver.

4. Results and discussion

We assembled an experimental setup following the scheme in figure 6 for a proof-of-concept demonstration of our system. The only microwave switch that we had available was a model limited to 65ns pulses, which set the maximum spatial resolution of the measurements to approximately 6m. However, as it was mentioned before, faster switches are commercially available so that even sub-meter resolution measurements should be possible with this system. The RF pulsed signal was measured in an electrical spectrum analyzer (ESA) at zero span as shown in figure 8(a). The ER level is found to be larger than 50dB. However, the measurement was limited by the ESA's noise floor. The extinction ratio given by the switch specifications is 60dB. In figure 8(a) the pulse shape is broadened due to the ESA's intermediate frequency filter bandwidth, 10MHz. An additional measurement was performed to check that clean, square pulses were been generated by using an optical detector and oscilloscope to measure the optical signal after FBG filtering. This is shown in figure 8(b), where a square pulse of 65ns duration is perfectly seen.

The ODSB-SC signal measured with an optical spectrum analyzer after the MZ-EOM is shown in figure 9. Also highlighted is the use of the FBG filter to obtain an optical single-sideband suppressed-carrier (OSSB-SC) signal for the gain configuration of the setup. The suppression of carrier and unwanted sideband relative to the wanted sideband were 38dB and 18dB, respectively. It is important to suppress the carrier as much as possible because it leads to Rayleigh scattering in the fibre in the same direction and at the same wavelength as the probe wave, which could have increased noise in detection. We checked that there was no problem with this in the measurement shown in figure 10. The received optical spectra with and without probe wave were measured to verify that spurious signals power could be neglected and further optical filtering in detection was unnecessary. The unwanted sideband suppression was also found to be enough to avoid the generation of Brillouin loss in the Stokes signal.

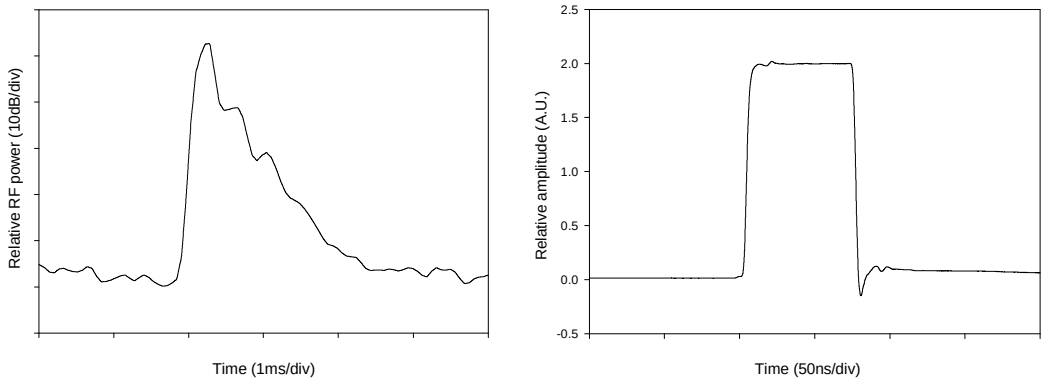

(a) (b)

Figure 8: (a) Measured RF pulse in the ESA at zero span. The pulse shape is distorted because of the limited bandwidth of the ESA (10MHz) and its dynamic range. (b) The optical pump pulse measured in an oscilloscope, where it is clearly seen that it is square and 65ns wide.

.

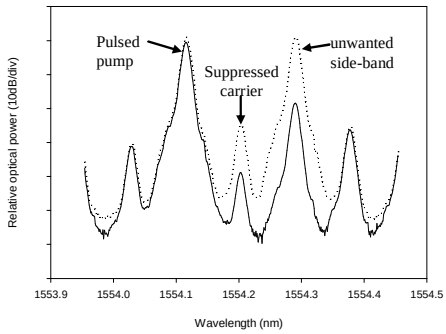

Figure 9: Effect of the FBG filtering of the OSDB-SC spectrum. The doted line corresponds to the signal before filtering and the solid line after. Previously published in [12].

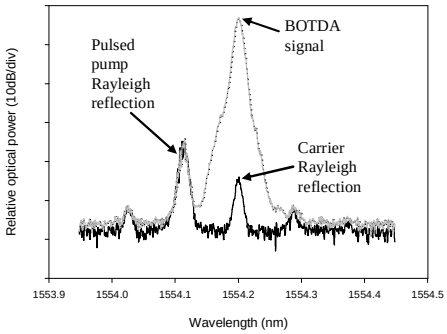

Figure 10: BOTDA signal spectra in detection measured is in grey. The dark line corresponds to Rayleigh scattering of the pump when the probe is switched off. Previously published in [12].

4.1. Measurements

We performed distributed temperature measurements in a 25-km length of standard single-mode fibre at 6-m resolution with 20-dBm pump pulses and -10-dBm CW. 200 m of the fibre were placed loose in a climatic chamber at 47ºC while the rest were held at room temperature in a reel. The RF was swept at 1-MHz steps.

The distributed measurement of the Brillouin spectra is shown in figure 11 after data processing (a Lorentzian fit). As explained in section 2.2 correction (7) is unnecessary in this measurements because the ER is so large

that the interaction between leakage and CW is negligible. The heated section of the fibre is clearly distinguishable due to the shift in the Brillouin frequency. After processing the temperature accuracy was estimated to be 0.44ºC in the worst case scenario with the heated section of the fibre at the end of the FUT, and was calculated with the standard deviation of the temperature measured in the heated section of the fibre shown in figure 12. The measurement of the frequency shift in the reel is not uniform because the fibre suffers random strain generated by the spool winding. The spatial resolution was confirmed to be 6m by measurements of rise time between two adjacent sections of fibre at different temperatures.

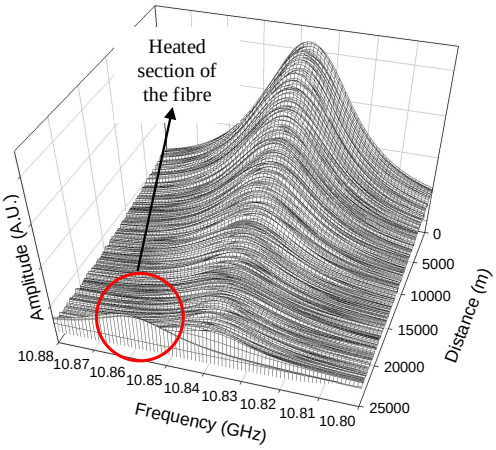

Figure 11: Evolution of the Brillouin spectra in the FUT. The heated section is clearly visible at the end and there is no measurement distortion due to the low leakage pulses.

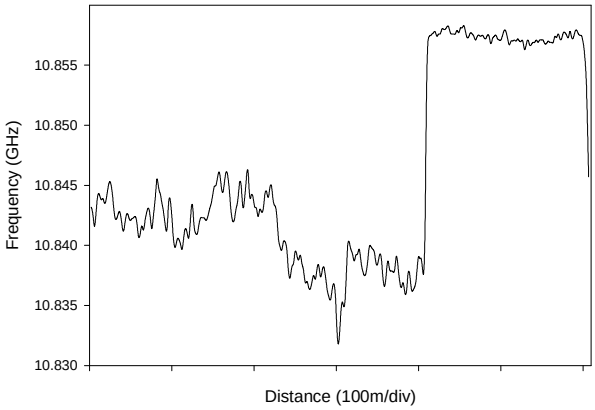

Figure12: Evolution of the measured Brillouin frequency shift in the end of the fibre. The last 200m correspond to the heated section of the fibre, where the measurement is very uniform.

4.2. Comparison of the system measurements with conventional systems with lower ER.

In order to compare our sensing scheme with the conventional schemes where lower extinction ratio pulses are launched into the FUT, we make some modifications in our experimental setup. We substitute the RF switch with a RF mixer, this way by introducing baseband pulses with a controlled level of DC, the pulsed RF signal after the mixer has an ER that can be controlled. This pulse shape is directly translated to the optical domain, so we can create pump pulses with similar ER as in the conventional BOTDA schemes, where the MZ-EOM directly pulses the optical carrier. Now we can vary the ER between 21dB and 28dB with the mixer and obtain up to 60-dB ER values when using the switch, as shown in figure 13. The spatial resolution has been modified to 19m in order to increase SBS gain, because the signal to noise ratio is much worse when lower ER pulses are used, since the interaction between CW and leakage adds a noisy DC level to the BOTDA signal. The gain of the EDFA is modified for every case so the pump pulse amplitude launched to the FUT is always the same, while the CW power is kept at -5dBm. The CW is also larger than previous measurements so as to gain some dynamic range in the measurements.

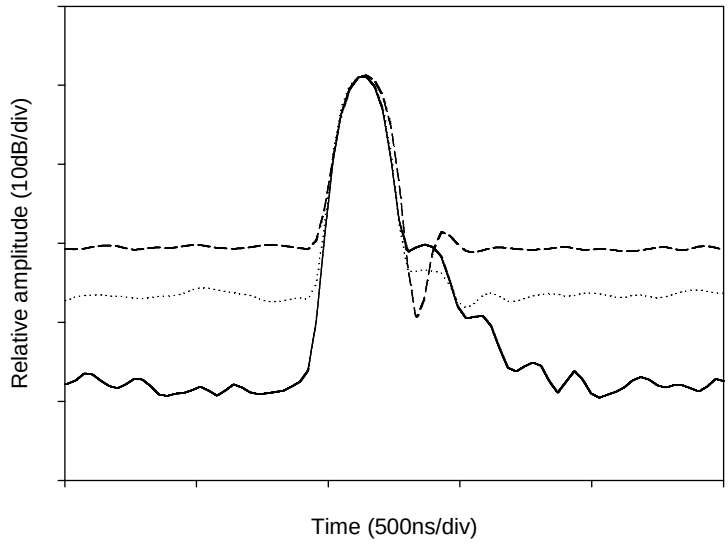

Figure 13: RF pulses with different ER level measured in the ESA at zero span. 21-dB ER in dashed line, 28-dB ER in dotted line and 60-dB ER in solid line. The pulse shapes are broadened because of the intermediate frequency of the ESA, the same as happens in figure 8(a). The measurement for the pulse with 60dB ER is limited by the ESA's dynamic range too, so the measured ER, 40dB, is worse than the given by the RF switch specifications, 60dB.

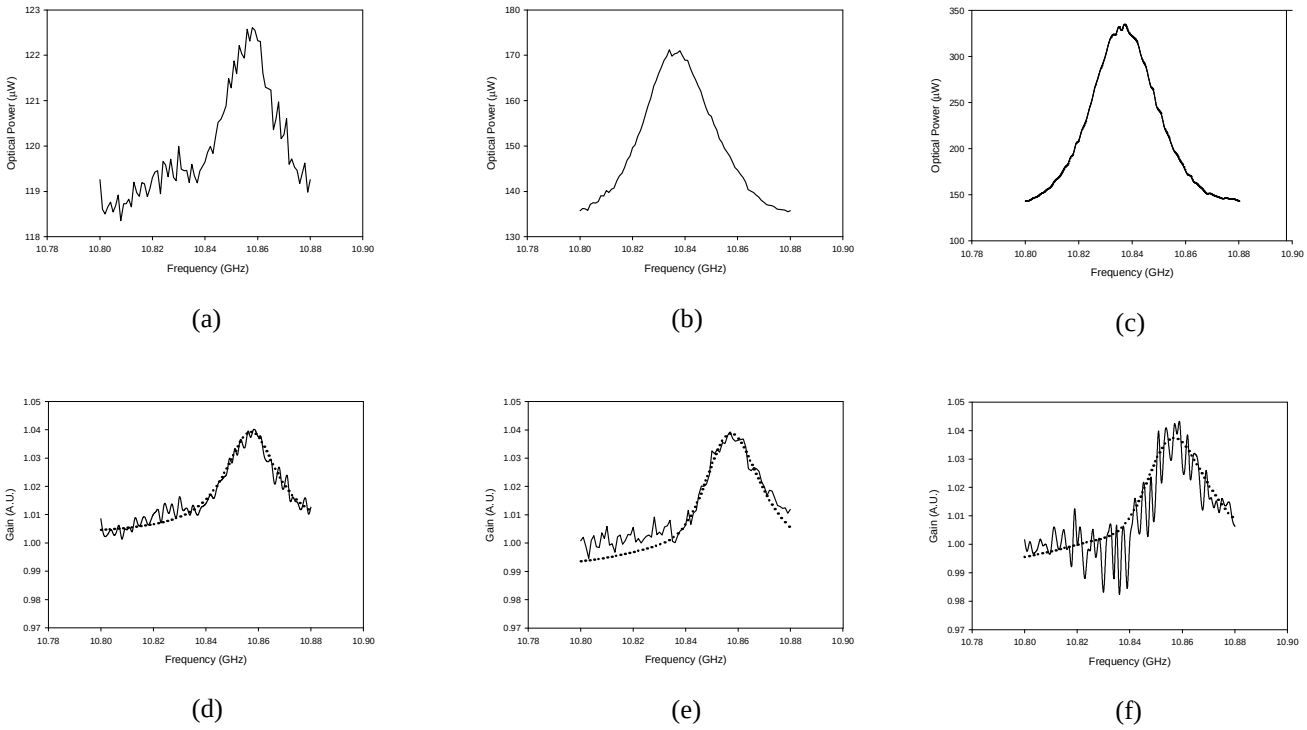

Figure14: Reconstructed spectra in the heated section for ER values of ER=60dB (a) without correction and (d) with correction; ER=28dB (b) without correction and (e) with correction; and ER=21dB (c) without correction and (f) with correction. The solid lines correspond to experimental measurements, while the dotted lines correspond to theoretical data calculated with the model described in section 2.

In figure 14 we observe the Brillouin spectra in the heated section of the fibre for different ER values of the pump pulses. In figure 14(a) to (c) no correction has been applied to the measurements. As predicted in section 2.2, only when we use 60-dB extinction ratio pulses the temperature is properly measured because the maxima of the gain corresponds to the frequency shift of the heated part. In contrast, when correction (7) is performed, in figures 14(d) to (f), we are able to measure the temperature shift with 21-dB and 28-dB ER. There is no need for correction (7) when 60dB ER pulses are used. This is because the spectrum of the interaction between leakage and CW is completely flat. So applying correction (7) is the same as dividing by a constant as has been explained in section 2.2. However this correction is also performed and the resulting trace is shown in figure 15(d) so as to compare with the measurements with lower extinction ratios.

In all three cases the traces match the theoretical model. Thus, the measurements show a 3MHz error for 21dB ER and 1.5MHz error for 28dB ER due to non-local effects. However, in the case of using the 60-dB ER pulses provided by our enhanced setup the error is lower than the frequency accuracy of the setting.

The traces 14 (d) to (f) are noisy, so the standard deviation of the experimental traces relative to the theoretical model was calculated. It grows as the leakage level increases: the larger leakage level, the greater the noise. This is attributed to the noisy DC level caused by the leakage-CW interaction, and cannot be suppressed with the correction.

Therefore, it is clearly beneficial to use our proposed scheme in long range BOTDA sensing shaping RF pulses in the electrical domain with a RF switch, since avoids errors caused by non-local effects and it is less noisy.

5. Conclusions

In this paper we have presented a new BOTDA sensor scheme that eliminates leakage in pump pulses. To study the benefits of leakage-free pump pulses in long range BOTDA sensing we have developed a theoretical model that includes leakage-CW interaction. We have found that the problem we avoid by suppressing the leakage is the distortion of the measured spectra. This distortion is greater for higher levels of leakage, because the interaction of the leakage with the CW raises the level of the second; hence a greater depletion of the pump pulse occurs, increasing the measurement error.

We have experimentally demonstrated our novel BOTDA configuration using RF shaping to obtain pump pulses with 60-dB extinction ratio. This extremely reduced leakage has been shown to completely suppress distortion of the measured spectra, thus sensor precision is enhanced, achieving a 0.44ºC accuracy sensor over 25km at 6m spatial resolution. Furthermore a simplified setup with a single MZ-EOM is deployed.

6. Acknowledgements

The authors wish to acknowledge financial support from the Spanish Ministerio de Educación y Ciencia through the project TEC2007-67987-C02-02, and from the Gobierno de Navarra through the research project 13.326.

7. References

[1] HORIGUCHI, T. and TATEDA, M., 1989. BOTDA - Non-destructive measurement of single-mode optical fibre attenuation characteristics using Brillouin interaction: Theory. Journal of Lightwave Technology, **7**, 1170-1176.

[2] NIKLÈS, M., THÉVENAZ, L. and ROBERT, P.A., 1997. Brillouin gain spectrum characterization in single-mode optical fibres. Journal of Lightwave Technology, **15**, 1842-1851.

[3] THÉVENAZ, L., LE FLOCH, S., ALASIA, D. and TROGER, J., 2004. Novel schemes for optical signal generation using laser injection locking with application to Brillouin sensing. Measurement Science and Technology, **15**, 1519-1524.

[4] LECŒUCHE, V., WEBB, D.J., PANNELL, C.N. and JACKSON, D.A., 1998. Brillouin based distributed fibre sensor incorporating a mode-locked brillouin fibre ring laser. Optics Communications, **152**, 263-268.

[5] LI, Y., BAO, X., RAVET, F. and PONOMAREV, E., 2008. Distributed Brillouin sensor system based on offset locking of two distributed feedback lasers. Applied Optics, **47**, 99-102.
[6] ALASIA, D., HERRÁEZ, M.G., ABRARDI, L., LÓPEZ, S.M. and THÉVENAZ, L., 2005. Detrimental effect of modulation instability on distributed optical fibre sensors using stimulated Brillouin scattering, 2005, pp587-590.
[7] DONG, Y., BAO, X., 2009. High spatial resolution and long-distance BOTDA using differential Brillouin gain in a dispersion shifted fiber, Proceedings of SPIE Vol 7503 (SPIE, Bellingham, WA, 2009), PDP 12, 20th International Conference on Optical Fibre Sensors. Edinburgh, U.K., 5-9 Oct. 2009.
[8] SOTO, M.A., BOLOGNINI, G. and DI PASQUALE, F., 2009. Enhanced simultaneous distributed strain and temperature fibre sensor employing spontaneous Brillouin scattering and optical pulse coding. IEEE Photonics Technology Letters, **21**, 450-452.
[9] GEINITZ, E., JETSCHKE, S., RÖPKE, U., SCHRÖTER, S., WILLSCH, R. and BARTELT, H., 1999. The influence of pulse amplification on distributed fibre-optic Brillouin sensing and a method to compensate for systematic errors. Measurement Science and Technology, **10**, 112-116.
[10] MINARDO, A., BERNINI, R., ZENI, L., THEVENAZ, L. and BRIFFOD, F., 2005. A reconstruction technique for long-range stimulated Brillouin scattering distributed fibre-optic sensors: Experimental results. Measurement Science and Technology, 16, 900-908.
[11] DIAZ, S., MAFANG, S.F., LOPEZ-AMO, M. and THÉVENAZ, L., 2008. A high-performance optical time-domain brillouin distributed fiber sensor. IEEE Sensors Journal, **8**, 1268-1272.
[12] ZORNOZA, A., OLIER, D., SAGUES, M., LOAYSSA, A., 2009. Distortion-free Brillouin distributed sensor using RF shaping of pump pulses, Proceedings of SPIE Vol 7503 (SPIE, Bellingham, WA, 2009), 75036D, 20th International Conference on Optical Fibre Sensors. Edinburgh, U.K., 5-9 Oct. 2009.
[13] AFSHAARVAHID, S., DEVRELIS, V. and MUNCH, J., 1998. Nature of intensity and phase modulations in stimulated Brillouin scattering. Physical Review A - Atomic, Molecular, and Optical Physics, **57**, 3961-3971.
[14] BAO, X., DHLIWAYO, J., HERON, N., WEBB, D.J. and JACKSON, D.A., 1995. Experimental and theoretical studies on a distributed temperature sensor based on Brillouin scattering. Journal of Lightwave Technology, **13**, 1340-1348.
[15] RAVET, F., BAO, X., LI, Y., YU, Q., YALE, A., KALOSHA, V.P. and CHEN, L., 2007. Signal processing technique for distributed Brillouin sensing at centimeter spatial resolution. Journal of Lightwave Technology, **25**, 3610-3618.
[16] KALOSHA, V.P., PONOMAREV, E.A., CHEN, L., and BAO, X., 2006. How to obtain high spectral resolution of SBS-based distributed sensing by using nanosecond pulses. Opt. Express **14**, 2071-2078.